Improved Transient Performance Properties of Distributed Generation Grid Side Converter Current Controller under Grid Voltage Harmonic Distortion and Unbalanced Faults

Zunaib Ali, Nicholas Christofides
Department of Electrical Engineering,
Frederick University,
Nicosia, Cyprus
zunaib.ali@stud.frederick.ac.cy,
n.christofides@frederick.ac.cy

Lenos Hadjidemetriou and Elias Kyriakides
Department of Electrical and Computer Engineering,
KIOS Research and Innovation Center of Excellence,
University of Cyprus,
Nicosia, Cyprus
[hadjidemetriou.lenos, elias]@ucy.ac.cy

Abstract- The fast and accurate control of renewable energy grid side converter (GSC) under normal and abnormal grid conditions is necessary to ensure the injection of high quality power and to enhance the power system stability. Accurate control of GSC is achieved by the stable and fast response of current and PQ controllers. In the event that the grid voltage becomes unbalanced due to the presence of grid harmonics or due to an unbalanced fault, the GSC should respond in such a way so as to inject balanced and harmonic free currents. If the inverter continues to generate a balanced harmonic free three-phase voltage, the resulting current will be unbalanced and harmonically distorted. It is therefore necessary to modify the three-phase voltage of GSC in accordance to grid disturbances. This paper proposes a current controller that improves the transient performance of the injected currents in the event of grid voltage harmonic distortion and unbalanced grid faults. The proposed harmonic neutralization current controller can inject high quality and pure sinusoidal positive sequence current accurately with faster harmonic compensation and improved dynamic response.

Keywords: Harmonic compensation, grid connected converter, SRF control, current controller.

I. INTRODUCTION

Renewable energy systems (RES) are nowadays extensively employed in order to meet the increasing demand of electrical power, to support the grid and to reduce dependency on depleting fossil fuels. The power produced by RES is effectively extracted and delivered to the grid by Grid Side Converter (GSC). The control GSC of mainly depends on the proper design of its control system. The control system of GSC consists of the outer active/reactive power controller, inner current controller and phase lock loop (PLL) [1, 2]. The outer control loop is referred as PQ controller and is employed for generating current references based on desired active/reactive power. The inner current control loop is responsible for accurate injection of provided references. The PLL is the heart of GSC control system, since it is used for the extraction of grid voltage phase angle [2]. The GSC control system can be further divided into two main control domains, the stationary αβ control fame and the synchronous reference frame (SRF). The αβ-domain control the voltage and currents as sinusoidal quantity with Proportional Resonant (PR) controller [3]. In contrast, PI controller is used in SRF domain for controlling the voltages/currents as DC quantities [4, 5]. In some cases, the two frames can be combined for even better performance [6-8], as employed in this paper. The performance of current controller is, however, affected by the off-nominal grid conditions, such as, unbalance grid faults, voltage sag/swell and grid voltage harmonic distortion [9-13]. Therefore, the design of current controller must be enhanced to cope with these disturbances.

Many current control techniques have been addressed in the literature. The simplest type of current controller is the SRF frame controller [1, 12], that employs a PI controller in fundamental positive SRF for injection of positive sequence current. The main disadvantage of this controller is that it cannot work accurately in the presence of unbalanced grid faults and grid voltage harmonics. The reason for inaccurate performance is that when a current signal containing harmonics and unbalance is rotated with SRF^{+1}, undesired frequency oscillations are observed on the transformed i_{dq}^{+1} vectors. For instance, an unbalance fault results in double frequency oscillations. The oscillations on i_{dq}^{+1} are not handled by the PI controller because it allows the accurate tracking of DC variables only. The inaccurate performance of SRF^{+1} controller under unbalance fault is mitigated by Dual SRF current controller [14, 15]. The Dual SRF controller employs two SRF frames, SRF^{+1} and SRF-1 respectively operating at $+\omega$ and $-\omega$. In addition to SRFs, some filters are also employed. The SRF^{+1} enables the injection of positive sequence and SRF^{-1} mitigates the undesired effect of unbalanced faults. The controller with filters in the control path results in slower dynamic response and furthermore, the unbalance faults are not fully mitigated.

The performance of Dual SRF controller is improved by enhanced dual SRF controller by introducing effective decoupling of oscillations resulted from transformed current

variables [16]. The computational complexity of the controller is high due to increased number of Park's transformation. Furthermore, the current controller requires undesired higher control effort because the voltage feedforward which plays an important role for SRF control is not used [17-19]. The Dual SRF controllers cannot compensate for harmonics as well.

The equivalent for PI controller in corresponding αβ is PR controller. The PR controller compensate for unbalanced grid fault due to the fact that it can compensate for reverse sequence of current at its own [7, 20], but it cannot work accurately in the presence of grid harmonics. Some interesting techniques are proposed in [21, 22], where hybrid version of PI and PR controller is employed for compensating the unbalanced grid faults. The controller in [8] combines a PI controller with several multi-resonant controllers for compensating the effect of harmonics and unbalanced faults. The controller, however, suffers from higher oscillations/overshoot in the event of unbalance fault [6]. In [23, 24], several SRF frames are combined to mitigate the selected lower order harmonics but unbalanced faults are not considered. The controller in [7] combines the PR controller with multi-SRFs from [23, 24] for allowing the accurate injection of current under unbalanced faults and grid harmonics. The fact that PR current controller does not allow the use of feedforward term, the current controller requires undesired control effort. Furthermore, the tuning of PR controller is not straightforward due to its higher order closed loop transfer function. The current controller in [18] employs unbalance and harmonic compensation unit together with conventional SRF^{+1} controller to deal with the problem of unbalance and harmonic distortion. The injected current, however, suffers from undesired oscillation due to inaccurate and slower harmonic compensation capability of the controller. The extended version of [18] is proposed in [17] to enable the simultaneous injection of both sequences of currents.

This paper proposes an advanced harmonic neutralization current controller that allows accurate injection of pure sinusoidal current with fast and accurate mitigation of grid voltage harmonic distortion. Furthermore, the proposed current controller improves the quality of injected current in the event of unbalanced fault by effective mitigation of undesired oscillations because of grid harmonics. The performance benchmarking of proposed technique is carried out with an existing state-of-the-art current controller.

II. Proposed Harmonic Neutralization Current Controller

The proposed current controller consists of SRF^{+1} controller for the accurate injection of fundamental positive sequence in the presence normal grid conditions. The additional unbalance and harmonic compensation modules for the mitigation of grid voltage unbalance faults and harmonic distortion. If these off-nominal grid conditions are not compensated, the injected GSC current contains unbalance and harmonic current components. The reason of this imbalancement and harmonics can be inferred from (1). If the grid voltage becomes unbalance (and/or harmonically distorted) and if GSC is still generating a balanced harmonic free three-phase voltage, the resulting current will be unbalanced and contains harmonics. It is therefore necessary to modify the three-phase voltage of GSC in accordance to grid disturbances. An important thing to mention is, the magnitude of unbalance current is higher because of unbalanced grid faults; however, the harmonic magnitude is less. Therefore, both the components are separately compensated. The current controller proposed in this paper mitigates the effect of unbalance by resonant current controller nested within the fundamental positive SRF controller and according to [6], selecting $h = 2$ in (2) allows accurate compensation.

$$\mathrm{i}_{abc} = \frac{v_{abc-GSC} - v_{abc}}{R_f + j\omega L_f} \qquad (1)$$

where, $v_{abc-GSC}$ is the voltage generated by GSC, v_{abc} is the three-phase grid voltage and ω is the nominal grid frequency.

$$G_R = \frac{K_R s}{s^2 + h\omega^2} \qquad (2)$$

where, K_R is the controller's proportional parameter.

The grid voltage harmonics are mitigated by a decoupling based novel structure referred as harmonic neutralization reference generator (HNRG), as shown in Fig. 1. In HNRG, the unbalanced and fundamental current components are separated from the measured grid current. The separated currents are subsequently subtracted from the actual measured current to get the resulting harmonic current components. The harmonic current is then multiplied with minus one to get the reverse of signal for neutralizing the effect of present harmonic currents due to grid voltage harmonics. The neutralization current is fed as a reference to the Harmonic Compensation Module (HCM). The HCM incorporates multi-SRFs along with integral controllers that modifies the GSC reference voltage in way to compensate the abnormal effect of grid harmonics. This neutralization phenomenon proposed in this paper results in very fast and accurate mitigation of harmonics compared to structure proposed in [18], where an error of measured and reference signal is to integral controller of compensation module. The steps for harmonic neutralization controller are:

1) The current measured signal is transferred to fundamental positive and negative sequence followed by a decoupling of double frequency oscillation.
2) The positive and negative extracted signals $\mathrm{i}_{\alpha\beta}^{+1}$ and $\mathrm{i}_{\alpha\beta}^{-1}$ are added together, thereby subtracted from measured current $\mathrm{i}_{\alpha\beta}$ to get the current containing only harmonics $\mathrm{i}_{\alpha\beta}^{h}$.
3) The $\mathrm{i}_{\alpha\beta}^{h}$ is multiplied with -1 and then treated as reference signal for injection, ultimately considered as harmonic compensation, since we are injecting opposite of what is present in the measured current signal.

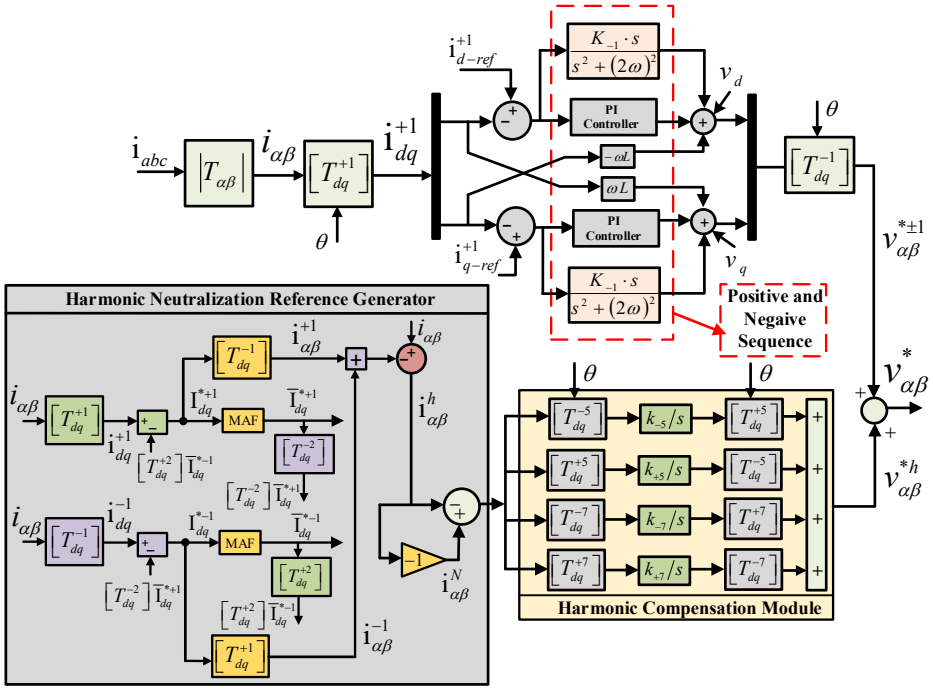

Fig. 1: Proposed harmonic neutralization current controller.

The separation of fundamental positive and negative current is enabled by the fact that when a signal rotated with a specific SRF speed, it contains significant oscillations because of other existing frequency components in the signal being rotated, as realized by (3), where n denotes the desired rotated frequency component vector and m are all other frequency components. As mentioned earlier, the unbalanced current component has significant magnitude, hence this component along with fundamental positive sequence component must be extracted. The fact that rotating a current signal containing fundamental and negative sequence component when rotated with SRF^{+1} results in 2ω oscillations and when rotated with SRF^{-1} results in -2ω oscillations, these oscillations must be decoupled from each other for accurate extraction of both sequences. The magnitude of oscillations for the case of SRF^{+1} equals to average magnitude of negative sequence component and vice versa, as given by (4). The rotation of SRFs is accomplished by phase angle extracted from grid voltage using an advanced EPMAFPLL Type 2 phase lock loop algorithm [4].

$$\mathrm{i}_{dq}^{n} = \underbrace{I^{n}\begin{bmatrix}\cos(\theta_n)\\ \sin(\theta_n)\end{bmatrix}}_{DC\ Term} + \underbrace{\sum_{m\neq n}\left\{I^{m}\left[\mathrm{T}_{dq}^{n-m}\right]\begin{bmatrix}\cos(\theta_m)\\ \sin(\theta_m)\end{bmatrix}\right\}}_{Oscillation} \quad (3)$$

$$\begin{bmatrix}\mathrm{i}_{dq}^{+1}\\ \mathrm{i}_{dq}^{-1}\\ \mathrm{i}_{dq}^{+5}\\ \mathrm{i}_{dq}^{-5}\end{bmatrix} = \begin{bmatrix}\mathrm{I}_{dq}^{+1}\\ \mathrm{I}_{dq}^{-1}\\ \mathrm{I}_{dq}^{+5}\\ \mathrm{I}_{dq}^{-5}\end{bmatrix} + \begin{bmatrix}[0] & T_{dq}^{+1-(-1)} & T_{dq}^{+1-(+5)} & T_{dq}^{+1-(-5)}\\ T_{dq}^{-1-(+1)} & [0] & T_{dq}^{-1-(+5)} & T_{dq}^{-1-(-5)}\\ T_{dq}^{+5-(+1)} & T_{dq}^{+5-(-1)} & [0] & T_{dq}^{+5-(-5)}\\ T_{dq}^{-5-(+1)} & T_{dq}^{-5-(-1)} & T_{dq}^{-5-(+5)} & [0]\end{bmatrix}\begin{bmatrix}\mathrm{I}_{dq}^{+1}\\ \mathrm{I}_{dq}^{-1}\\ \mathrm{I}_{dq}^{+5}\\ \mathrm{I}_{dq}^{-5}\end{bmatrix} \quad (4)$$

where, $\left[T_{dq}^{n}\right]$ represents Park's transformation.

The decoupling equation is given by (5), by neglecting harmonics. The harmonics as mentioned are neglected in (5) for instance just to calculated the positive and negative sequences, because due to smaller magnitude it only originates lower oscillations on transformed DC positive and negative sequence components, which when passed through a moving average filter (MAF), acting as low pass filter (LPF)), are suppressed. According to [25], moving average filter ensures high noise suppression capability. The MAF acts as an ideal LPF under certain conditions and have linear-phase. The z-domain transfer function of MAF based LPF is given by (6). The discrete implementation of MAF can be realized by one multiplication, one addition and one subtraction. It is worth mentioning that harmonics are neglected in this step only to enable the extraction of positive and negative sequence, and ultimately the extracted components are being utilized by HCM for a complete suppression of harmonics. The resulting signals are transformed back to αβ-domain and subtracted from actual measured current resulting in current with harmonics only, as shown in (7). The neutralization current is denoted by $\mathrm{i}_{\alpha\beta}^{N} = -\mathrm{i}_{\alpha\beta}^{h}$. The error of $\mathrm{i}_{\alpha\beta}^{h}$ and $\mathrm{i}_{\alpha\beta}^{N}$ is subsequently transfer to HCM for compensation of harmonics.

$$\begin{bmatrix}\mathrm{I}_{dq}^{*+1}\\ \mathrm{I}_{dq}^{*-1}\end{bmatrix} = \begin{bmatrix}\mathrm{i}_{dq}^{+1}\\ \mathrm{i}_{dq}^{-1}\end{bmatrix} - \begin{bmatrix}[0] & T_{dq}^{+1-(-1)}\\ T_{dq}^{-1-(+1)} & [0]\end{bmatrix}\begin{bmatrix}\bar{\mathrm{I}}_{dq}^{*+1}\\ \bar{\mathrm{I}}_{dq}^{*-1}\end{bmatrix} \quad (5)$$

$$F_{MAF}(z) = \frac{1}{N}\frac{1-z^{-N}}{1-z^{-1}} \quad (6)$$

Where, N relates to size of MAF window.

$$\mathrm{i}^{h}_{\alpha\beta} = \mathrm{i}_{\alpha\beta} - \underbrace{\mathrm{I}^{*+1}_{dq}\left[T^{-1}_{dq}\right]}_{\mathrm{i}^{+1}_{\alpha\beta}} - \underbrace{\mathrm{I}^{*-1}_{dq}\left[T^{+1}_{dq}\right]}_{\mathrm{i}^{-1}_{\alpha\beta}} \quad (7)$$

where, I^{*+1}_{dq} and I^{*+1}_{dq} are estimated positive and negative sequence of measured current, and $\bar{\mathrm{I}}^{*\pm1}_{dq}$ is filtered estimated vectors.

Furthermore, the proposed harmonic neutralization scheme also improves the performance of current controller under unbalanced grid faults in the presence of harmonic distortion. In contrast, the current controller in [18] cannot fully mitigates the undesired effect of harmonic in the presence of unbalanced grid fault.

III. Tuning Of Proposed Current Controller

The tuning of proposed current controller can be divide into two separate tuning cases due to reason that the dynamics of conventional PI employed in SRF frame are independent from the R and I controllers employed for unbalance and harmonic mitigation. The PI controller tuning is done based on the closed loop control system equivalent of proposed current controller, shown in Fig. 2. The tuning of PI is enabled by considering the transfer function of PI controller $G_{PI}(s) = k_p + \frac{1}{T_i}\frac{1}{s}$, with k_p and T_i as PI parameters, the L-type approximated transfer function of LCL filter $G_f(s) = \frac{1}{R_f + L_f s}$ (L_f and L_f is inductance and resistance of filter, respectively), and the transfer function for control delays $G_{PD}(s) = \frac{1}{1+T_d s}$. The closed loop transfer function corresponding to Fig. 2 is given by (8), where i is current injected by GSC and i_r is reference current.

$$H_C(s) = \frac{i}{i_r} = \frac{\left(\frac{k_p T_i s + 1}{T_i s}\right)\left(\frac{1}{1+T_d s}\right)\left(\left({}^{1}/_{R_f}\right)\Big/\left(1+\frac{L_f}{R_f}s\right)\right)}{1+\left(\frac{k_p T_i s + 1}{T_i s}\right)\left(\frac{1}{1+T_d s}\right)\left(\left({}^{1}/_{R_f}\right)\Big/\left(1+\frac{L_f}{R_f}s\right)\right)} \quad (8)$$

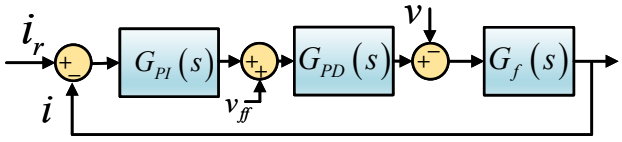

Fig. 2: Closed-loop system for current controller.

The solution to transfer function of (9) by the selection of the term $k_p T_i$ equal to ${}^{L}/_{R}$ is given as the solution of second-order transfer function (9), and resulting parameters are shown in (10). The damping factor ζ is selected as 0.707 for optimally damped response of the second order transfer function.

$$H_C(s) = \frac{\omega_n^2}{s^2 + 2\zeta\omega_n s + \omega_n^2} = \frac{\left(\frac{1}{T_i T_d R}\right)}{s^2 + \left(\frac{1}{T_d}\right)s + \left(\frac{1}{T_i T_d R}\right)} \quad (9)$$

$$k_p = \frac{L}{2T_d} \text{ and } T_i = \frac{2T_d}{R} \quad (10)$$

where T_d shows the amount of overall delay experienced in control path. Delay can be caused because of computation devices, PWM generator or any other. The optimal value of T_d according [17] is $5T_s$, where T_s denotes the sampling period used for GSC controller.

The resonant and integral controllers are tuned based on the fact that harmonics and unbalance have different dynamics. The unbalance faults occur with fast dynamics; hence the resonant gain must be higher (5000). However, the I controller are tuned at lower value (1200) of tuning parameter due to slower dynamics of harmonic components.

IV. Frequency Domain Analysis

The transfer function of HNRG according to (11) is given by (12) and bode diagram is shown in Fig. 3. The positive and negative sequence fundamental components completely are blocked, while passing all the remaining harmonic components.

$$\frac{i^{h}_{\alpha\beta}}{i_{\alpha\beta}} = \frac{1-[TFT^{-1}]}{1-[TFT^{-1}]TFT^{+1}} + \frac{1-[TFT^{+1}]}{1-[TFT^{+1}]TFT^{-1}} \quad (11)$$

$$TFT^{k} = \left[T^{-k}_{dq}\right][F(s)]\left[\mathrm{T}^{k}_{dq}\right] = \frac{\omega_f}{s+(\omega_f - j\cdot k\cdot\omega)} \quad (12)$$

where, $\omega = 2\pi 50$ rad/s is grid nominal frequency and ω_f is the cutoff frequency of LPF.

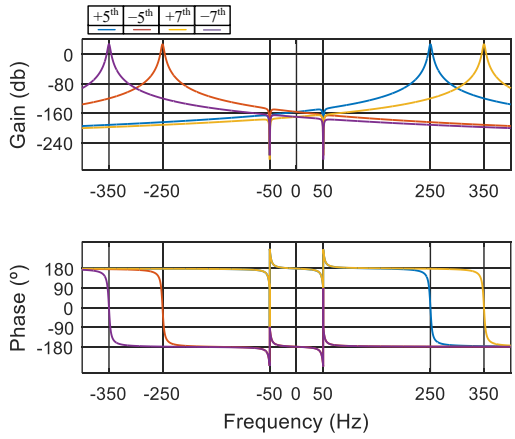

Fig. 3: Frequency response of proposed harmonic neutralization current controller.

The output of HNRG is provided as an input to HCM. Consequently, the transfer function of (11) is further multiplied with (12) for each sub-harmonic compensation module (with k=+5, -5, +7, -7) and resulting bode is shown in Fig. 3. As can be seen, specific harmonic component is passed by each sub-module of HCM with positive gain and zero phase shift, while all other frequency components are blocked. The passed error component is subsequently compensated by the integral action of I controller and corresponding voltage signal is generated for PWM of GSC.

V. Results And Discussion

The performance of proposed current controller is compared with [18] in terms of improved harmonic compensation for proposed controller due to neutralization phenomenon. The two current controller are tuned for similar tuning parameters. The conventional and unbalance compensation parts for both current controllers are made similar in order for analyzing the improved performance in terms of harmonic compensation explicitly. Simulation and experiments are performed for validating the improved performance of new proposed harmonic neutralization current control technique. The simulation and experimental setups are identical and are developed according to the schematic shown in Fig. 4. The proposed current controller is referred as Neutralization controller (NC) and controller of [18] is referred as existing controller (EC).

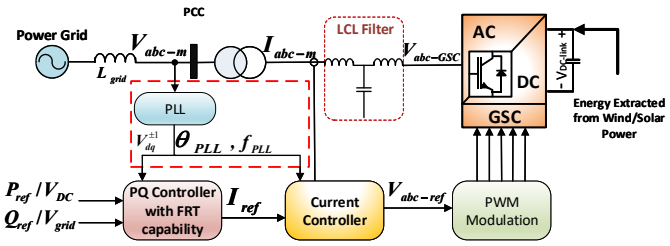

Fig. 4: Schematic of grid connected RES system.

A. Simulations Results

The first comparison is developed for the case of grid voltage harmonic distortion. The initial reference value for i_d^{+1} and i_q^{+1} is set to 4.5A and 2A, respectively. Initially the grid voltage is normal containing fundamental positive sequence voltage. However, at t=0.8 sec the grid voltage is injected with +5th and -7th harmonic with respective magnitudes of 0.09 pu and 0.08 pu. The harmonics are injected but the harmonic compensation module for both the controller is not activated until t=1 sec. As can be observed from Fig. 5 that after t=1 sec when the harmonic compensation is enabled, the proposed harmonic neutralization current controller works fast and quickly mitigates the undesired effect of harmonic distortion within 0.05s of time. In contrast, the existing controller (EC) takes too much time, approximately 0.15 sec, to overcome the effect of harmonics. The proposed harmonic compensation controller is more efficient in terms of faster harmonic compensation as compared to the other existing harmonic compensation technique.

The second case study analyzes the behavior of proposed current controller and compares it with the existing current controller under harmonics and unbalance fault. The harmonic conditions are similar to the previous case study, that is, +5th and -7th harmonic are injected with magnitudes of 0.09 pu and 0.058 pu, respectively. The injection harmonic is enabled at t=0.6 sec and improved performance of proposed current controller similar to previous case study can be seen from Fig. 6. This case study is carried out specially to witness the performance improvement of proposed current controller in the event unbalanced grid fault together with harmonic distortion. The unbalanced Type C fault occurs at t=0.8 sec. The controller of [18] undergoes oscillation and the effect of harmonics is not fully mitigated. As can be seen that the EC takes 0.1 sec to overcome the problem of harmonics after the fault is applied. However, on the other hand, the proposed current controller improves the quality of inject current by improving the controller's response, lower oscillations and faster mitigation of undesired harmonics. The results demonstrated in Fig. 6, validates the accurate and faster response of proposed current controller.

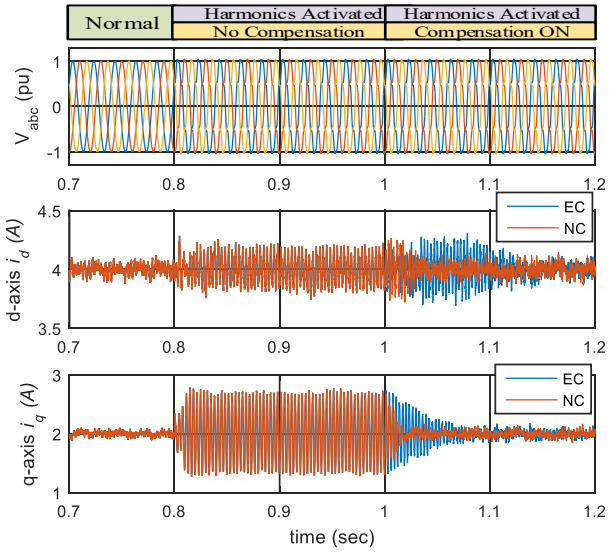

Fig. 5: Comparative performance under grid voltage harmonic condition.

The proposed harmonic neutralization current controller can inject high quality and pure sinusoidal positive sequence current accurately with faster harmonic compensation, and improved performance. Thus, the proposed current controller can ensure the safe and appropriate operation of the GSC and RES according to the modern grid regulations.

B. Experimental Results

The proposed current controller is validated through experiments and results are presented in Fig. 7. The grid voltage is unbalanced and also it contains 5th, 7th, -11th and 13th harmonic. The HCM is enabled from the start, whereas the unbalanced module is activated later, as shown in Fig. 7. The three-phase currents injected by the proposed current controller are asymmetrical but harmonic free. However, when the unbalance module is activated, the three-phase current becomes symmetrical as well. The i_d^{+1} in Fig. 7 (b) contains 2ω oscillations until the R-controller is activated to compensate. This validates the quality enhancement of injected current by GSC under harmonic-distorted and unbalanced grid conditions.

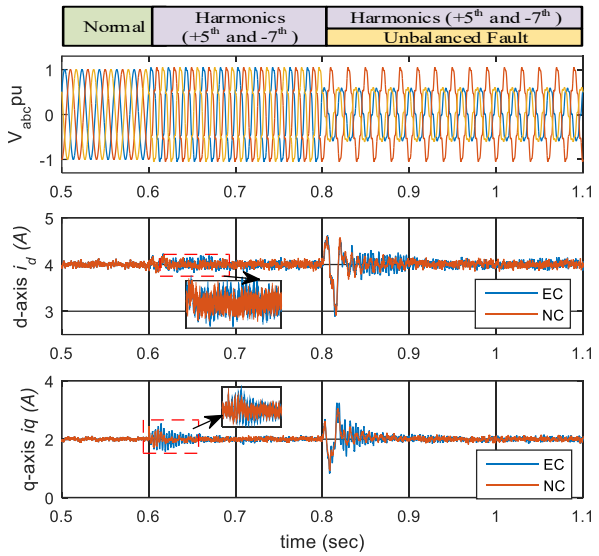

Fig. 6: Comparative performance under harmonic and unbalance fault conditions.

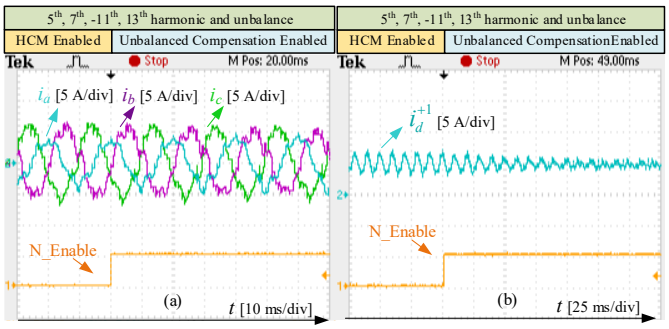

Fig. 7: Experimental verifications for the proposed harmonic neutralization current controller.

VI. Conclusion

The proposed current controller has improved transient performance when mitigating the grid voltage harmonics and unbalance faults as a result of a new harmonic neutralization topology. The performance enhancement of the proposed controller is verified through simulation and experimental results. The proposed current controller can be therefore used for fault ride through operation of grid connected RES systems.

Acknowledgement

Author Ali is grateful to Erasmus Mundus for providing PhD fellowship; Hadjidemetriou and Kyriakides acknowledge financial support by Cyprus Research Promotion Foundation.

References

[1] R. Teodorescu, M. Liserre, and P. Rodriguez, *Grid converters for photovoltaic and wind power systems*. USA: Wiley-IEEE Press, 2011.

[2] Z. Ali, N. Christofides, L. Hadjidemetriou, and E. Kyriakides, "A New MAF based αβEPMAFPLL for Grid Connected RES with Improved Performance under Grid Faults," *Electric Power Systems Research,* vol. 154C pp. 130-139, August, 2017.

[3] P. Rodrdguez, A. Luna, A. R. S. Muoz, , R. Teodorescu, and F. Blaabjerg, "A stationary reference frame grid synchronization system for three-phase grid-connected power converters under adverse grid conditions," *IEEE Trans. Power Electronics,* vol. 27, no. 1, pp. 99-112, 2012.

[4] Z. Ali, N. Christofides, L. Hadjidemetriou, and E. Kyriakides, "Performance enhancement of MAF based PLL with phase error compensation in the pre-filtering stage " in *Proc. IEEE PowerTech*, Manchester, 2017, pp. 1-6.

[5] Z. Chen, J. M. Guerrero, and F. Blaabjerg, "A review of the state of the art of power electronics for wind turbines," *IEEE Trans. Power Electronics,* vol. 24, no. 8, pp. 1859-1875, 2009.

[6] Z. Ali, N. Christofides, and A. Polycarpou, "Performance enhanced RES current controller with reduced computational complexity," in *Proc. IEEE MPS*, Romania, 2017, pp. 1-6.

[7] Z. Ali, N. Christofides, L. Hadjidemetriou, and E. Kyriakides, "An advanced current controller with reduced complexity and improved performance under abnormal grid conditions " in *Proc. IEEE PowerTech*, Manchester, 2017, pp. 1-6.

[8] M. Liserre, R. Teodorescu, and F. Blaabjerg, "Multiple harmonics control for three-phase grid converter systems with the use of PI-RES current controller in a rotating frame," *IEEE Trans. Power Electronics,* vol. 21, no. 3, pp. 836-841, 2006.

[9] Z. Ali *et al.*, "Generalized method for harmonic elimination in two and three level voltage sourced converters," in *Proc. IEEE ICET*, 2015.

[10] "IEEE Standard for Interconnecting Distributed Resources with Electric Power Systems," *IEEE Std 1547-2003,* pp. 1-28, 2003.

[11] F. Blaabjerg, M. Liserre, and K. Ma, "Power electronics converters for wind turbine systems," *IEEE Trans. Industry Applications,* vol. 48, no. 2, pp. 708-719, 2012.

[12] M. Altin, O. Goksu, R. Teodorescu, P. Rodriguez, B. B. Jensen, and L. Helle, "Overview of recent grid codes for wind power integration," in *Proc. IEEE OPTIM*, 2010, pp. 1152-1160.

[13] F. Blaabjerg, R. Teodorescu, and A. V. Timbus, "Overview of control and grid synchronization for distributed power generation systems," *IEEE Trans. Industrial Electronics,* vol. 53, no. 5, pp. 1398-1409, 2006.

[14] S. Yongsug and T. A. Lipo, "Control scheme in hybrid synchronous stationary frame for PWM AC/DC converter under generalized unbalanced operating conditions," *IEEE Trans. Industry Applications,* vol. 42, no. 3, pp. 825-835, 2006.

[15] S. Hong-Seok and N. Kwanghee, "Dual current control scheme for PWM converter under unbalanced input voltage conditions," *IEEE Trans. Industrial Electronics,* vol. 46, no. 5, pp. 953-959, 1999.

[16] M. Reyes, P. Rodriguez, S. Vazquez, A. Luna, R. Teodorescu, and J. M. Carrasco, "Enhanced decoupled double synchronous reference frame current controller for unbalanced grid-voltage conditions," *IEEE Trans. Power Electronics,* vol. 27, no. 9, pp. 3934-3943, 2012.

[17] Z. Ali, N. Christofides, L. Hadjidemetriou, and E. Kyriakides, "A computationally efficient current controller for simultaneous injection of both positive and negative sequences," in *Proc. IEEE ECCE Europe*, Warsaw Poland, 2017, pp. 1-6.

[18] L. Hadjidemetriou, E. Kriakides, and F. Blaabjerg, "A grid side converter current controller for accurate current injection under normal and fault ride through operation," in *Proc. IEEE IECON*, 2013, pp. 1454-1459.

[19] Z. Ali, N. Christofides, L. Hadjidemetriou, and E. Kyriakides, "Diversifying the role of distributed generation grid side converters for improving the power quality of distribution networks using advanced control techniques," in *Proc. IEEE ECCE USA*, 2017, pp. 1-6.

[20] R. Teodorescu, F. Blaabjerg, and M. Liserre, "Proportional-resonant controllers. A new breed of controllers suitable for grid-connected voltage-source converters," in *Proc. IEEE OPTIM*, 2004.

[21] C. Wessels, N. Hoffmann, and F. Fuchs, "StatCom control at wind farms with fixed-speed induction generators under asymmetrical grid faults," *IEEE Trans. Industrial Electronics,* vol. 60, no. 7, pp. 2864-2873, 2013.

[22] J. Hu, Y. He, L. Xu, and B. W. Williams, "Improved control of DFIG systems during network unbalance using PI&R current regulators," *IEEE Trans. Industrial Electronics,* vol. 56, no. 2, pp. 439-451, 2009.

[23] M. J. Newman, D. N. Zmood, and D. G. Holmes, "Stationary frame harmonic reference generation for active filter systems," *IEEE Trans. Industry Applications,* vol. 38, no. 6, pp. 1591-1599, 2002.

[24] V. T. Phan and H. H. Lee, "Control strategy for harmonic elimination in stand-alone dfig applications with nonlinear loads," *IEEE Trans. Power Electronics,* vol. 26, no. 9, pp. 2662-2675, 2011.

[25] S. Golestan, F. D. Freijedo, A. Vidal, J. M. Guerrero, and J. Doval-Gandoy, "A quasi-type-1 phase-locked loop structure," *IEEE Trans. Power Electronics,* vol. 29, no. 12, pp. 6264-6270, 2014.